AN EFFICIENT METHOD FOR GENERATING QUANTUM ENTANGLED PHOTON PAIRS

Jeerasak PHU-ARPHIT[1], Thanapat PHETVONGSAKUL[1], Ruchipas BAVONTAWEEPANYA[1], Atirach RITBOON[1] and Ekkarat PONGOPHAS[1*]

1 Division of Physics, Faculty of Science and Technology, Thammasat University, Thailand; e_pong@tu.ac.th (Corresponding Author)

ARTICLE HISTORY
Received: 9 June 2025 **Revised:** 23 June 2025 **Published:** 7 July 2025

ABSTRACT

Quantum entanglement plays a crucial role in quantum information science, particularly in quantum teleportation and the development of quantum key distribution (QKD). It is a phenomenon in which the quantum state of each particle in a pair or a group of particles is correlated to others and cannot be described independently. In this study, we demonstrate a simplified experimental setup for generating entangled photon pairs using spontaneous parametric down-conversion (SPDC) in a beta barium borate (BBO) crystal. A paper mask, designed to fit a down-converted photon path, crucially simplifies the alignment of optical components, leading to a significant improvement in the placement of detectors. The state of the generated entangled photons is then measured by two detectors equipped with polarization filters, to examine the correlation of the entangled photons. The coincidence counts were measured while varying the rotation angles of the polarizers. The first polarizer was oriented at 0°, 45°, 90°, and 135° relative to the vertical axis, while the second polarizer was rotated in 15° increments starting from 0°. The Bell-CHSH inequality test was performed, yielding an $S = 2.709 \pm 0.083$, indicating strong quantum entanglement. This practical approach for generating entangled photon pairs offers simplicity while achieving strong entanglement, which is essential for quantum communication applications.

Keywords: Quantum Entanglement, Bell-CHSH Inequality, Parametric Down-Conversion

CITATION INFORMATION: Phu-arphit, J., Phetvongsakul, T., Bavontaweepanya, R., Ritboon, A., & Pongophas, E. (2025). An Efficient Method for Generating Quantum Entangled Photon Pairs. *Procedia of Multidisciplinary Research, 3*(7), 46.

INTRODUCTION

Quantum entanglement is a phenomenon where states of two or more particles become correlated to each other in such a way that cannot be described with classical probability theory. It is only the total state of these particles that can give a complete description about their statistics of measurements (Horodecki et al., 2009). Measurement of one particle state instantly influences the state of the other, regardless of distance through wave function collapse. Such non-classical properties offer benefits across various fields of quantum processing and information. More specifically, quantum entangled photons can be used to develop photonic quantum computers to perform complex calculations exponentially faster than their classical counterparts (Kimble, 2008; O'Brien et al., 2009). Entangled photons enable quantum key distribution (QKD), as in the case of the E91 protocol, ensuring ultra-secure communication. Any eavesdropping attempt disturbs the entangled state, signaling Alice and Bob, the two involved parties, about the existence of the eavesdroppers in the communication network (Gisin et al., 2002; Scarani et al., 2009). Entangled photons can enhance the sensitivity of sensors, improving technologies like GPS, medical imaging, and gravitational wave detection (Xia et al., 2020; Giovannetti et al., 2011). The development of techniques to produce quantum entanglement states is therefore essential for the development of quantum technologies.

In quantum optics, the most common technique to produce entangled photon pairs is spontaneous parametric down-conversion (SPDC), when a nonlinear crystal BBO is pumped with a high-energy laser beam (typically ultraviolet or blue light). When a pump photon interacts with the crystal, it is converted into two lower-energy photons, the so-called signal and idler photons, due to the frequency and phase-matching condition. This phase-matching condition determines the precise directions of signal and idler photons emitted from the crystal. Thus, collecting detectors together with other optical components need to strategically align to capture both photons emitted along these specific directions. Setting up the optical system for invisible down-conversion photon pairs, as in this work, becomes very challenging as the experimentalists cannot see the down converted photons' path during the setup. In such cases, we need proper optical alignment techniques to achieve a sufficiently high photon flux.

This paper describes a simple yet low-cost technique for the optical alignment needed to collect photon pairs generated by a pair of 5mm x 5mm x 0.5mm type-I BBO crystal. The pump laser is a continuous wave 80-mW, 405-nm laser diode. These crystals are designed to produce 810 nm degenerate entangled photon pairs emitted at an angle of ±3° with respect to the pump beam. As the 810 nm down-converted entangled photons are invisible, we employed the guiding lasers together with a designed paper mask with three pre-calculated position holes to resolve the invisible difficulty and achieve an effective optical setup. The distinct advantages in terms of simplicity, performance, and flexibility of this method are demonstrated and discussed in this paper.

METHODS

Optical setup

To establish the experimental setup for spontaneous parametric down-conversion (SPDC), the following procedure is employed. First, the heights of iris diaphragms 1, 2, and 3 are adjusted to ensure coplanarity. Second, iris diaphragms 1 and 3 are aligned along an optical main path, as depicted in Figure 2. A laser beam from a 450 nm laser diode is then directed through iris diaphragms 1 and 3 by reflecting off a silver mirror and a polarizing beam splitter (PBS) to select only the vertically polarized component to be in the optical main path. This reflected beam from the PBS is adjusted to pass through iris diaphragms 1 and 3, ensuring precise alignment. Following beam alignment, iris diaphragm 2 is placed in the optical main path, serving as a reference point for the BBO crystal. A 3-degree measuring screen, as shown in Figure 1, serving as optical apertures corresponding to the photon pair positions generated via

SPDC from a beta-barium borate (BBO) crystal, is positioned 21 cm from iris diaphragm 2. This distance corresponds to the location at which a light beam diverges at ±3 ° relative to the pump beam can pass through the measuring screen with three apertures separated by 1.1 cm. The position of the 3-degree measuring screen is aligned in a way that the pump beam passes through the central aperture. Two guiding lasers are directed through the left-side and right-side apertures of the 3-degree measuring screen and iris diaphragm 2. Then, a fiber-optic collimator lens is precisely positioned along the alignment laser path to collect the down-converted photon pairs. The down-converted photons are then transmitted to two avalanche photodiodes (APD) via optical fibers. To optimize this alignment, we used a power meter to measure the intensity of alignment laser light exiting the fiber, with adjustments made to maximize the intensity. Two 750 nm long-pass filters are installed in front of the fiber-optic collimators, followed by polarizer 1 (POL1) and polarizer 2 (POL2).
Subsequently, a half-wave plate (HWP) and a quarter-wave plate (QWP) are sequentially positioned after the 3-degree measuring screen. Finally, the iris diaphragm 2 is replaced by the BBO crystal, as illustrated in Figure 3. This configuration highlights the utility of the 3-degree measuring screen, constructed from paper, which can be readily fabricated and positioned at any desired distance for SPDC experiments.

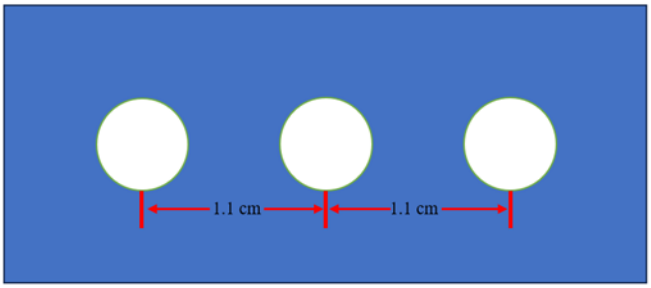

Figure 1 3-degree measuring screen with three apertures separated by 1.1 cm

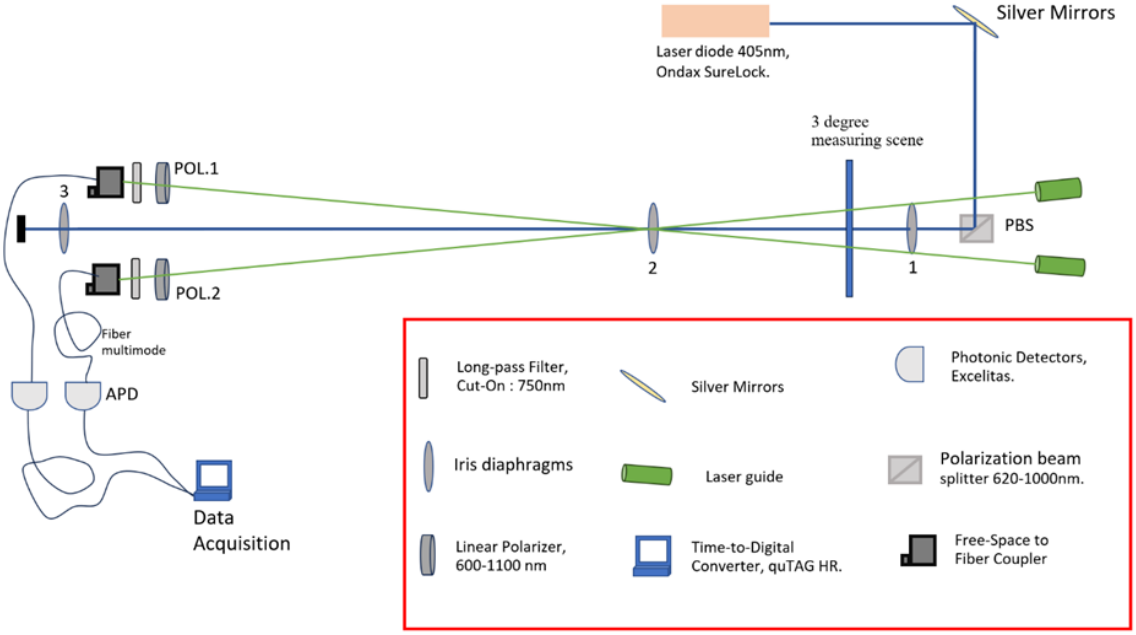

Figure 2 The alignment of the 405 nm laser diode beam using iris diaphragms and guiding lasers for positioning the collimator lens.

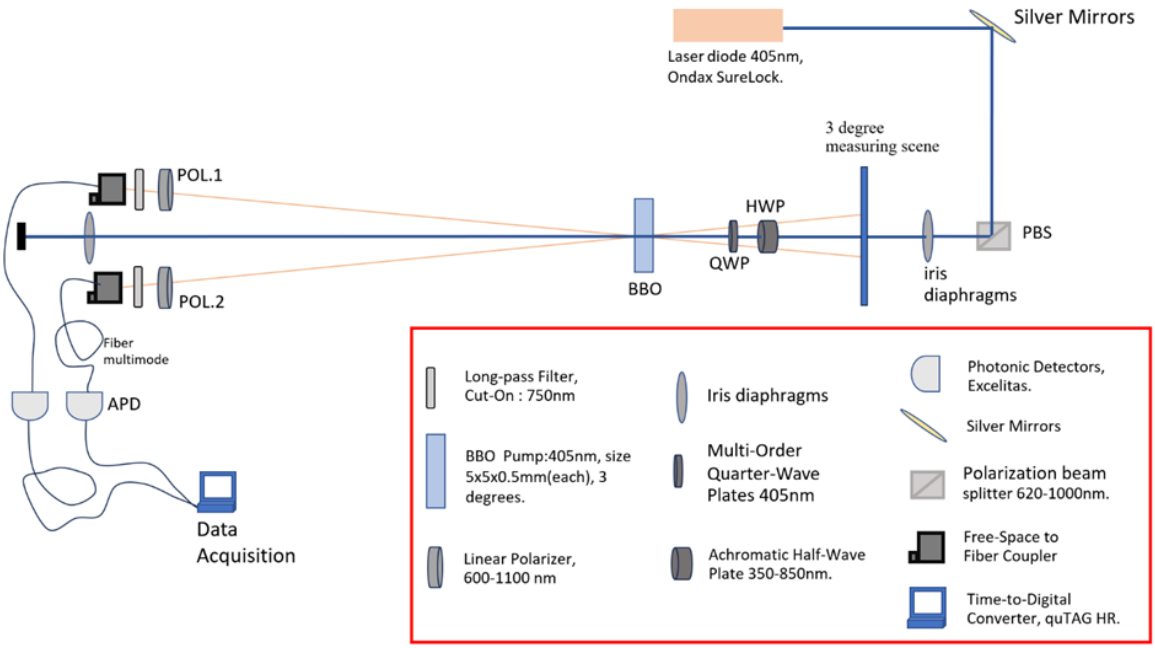

Figure 3 The experimental setup for measuring the correlation.

The laser beam emitted from the laser diode is reflected by a polarizing beam splitter (PBS), giving us a vertically polarized beam. When this vertically polarized beam passes through a half-wave plate (HWP) set at an angle of 22.5° relative to the vertical direction, the polarization state of the photon becomes

$$|\psi\rangle = \frac{1}{\sqrt{2}}(|V\rangle + |H\rangle). \quad (1)$$

These pump photons then enter a nonlinear down-conversion crystal, a type I beta-barium borate (BBO) crystal. Through the process of spontaneous parametric down-conversion (SPDC), high-energy photons are converted into pairs of lower-energy photons with specific polarization correlations. As a result, a vertically polarized photon of the pump beam is down-converted into two horizontally polarized photons,

$$|V\rangle \rightarrow |H\rangle|H\rangle, \quad (2)$$

While a horizontally polarized photon on the other hand is down-converted into two vertically polarized photons,

$$|H\rangle \rightarrow |V\rangle|V\rangle. \quad (3)$$

Since the polarization state of the photons in the pump beam, shown in Equation (1), is an equal superposition of vertical and horizontal components, both down-conversion processes occur with an equal probability. However, due to the birefringence and finite thickness of the BBO crystal, a temporal delay is introduced between horizontally and vertically polarized photons. To compensate for this temporal delay and ensure the indistinguishability between the two polarization paths, a quarter-wave plate (QWP) is placed after the BBO crystal. This enables the generation of a polarization-entangled Bell state:

$$|\Phi^+\rangle = \frac{1}{\sqrt{2}}(|H\rangle|H\rangle + |V\rangle|V\rangle) \quad (4)$$

To verify the generation of the $|\Phi^+\rangle$ entangled state, we measured polarization correlations in the diagonal basis. Specifically, we verified whether the coincidence counts in the anti-correlated diagonal polarization states $|+45°\rangle|-45°\rangle$ and $|-45°\rangle|+45°\rangle$ are minimized. This can be accomplished by setting polarizer 1 at +45° and Polarizer 2 at -45° relative to the vertical axis and then adjusting the QWP angle until the coincidence count reaches its minimum value. This minimization of coincidences in the anti-diagonal basis serves as an indicator that the photon pair is in the desired $|\Phi^+\rangle$ entangled state.

Correlation predictions

In this experimental setup, the two polarizers placed in front of the detectors are rotated to various angles, denoted as α and β. For the photon detections, each photon is found to be in either the positive or negative polarization state in the rotated basis

$|+\alpha\rangle,\ |-\alpha\rangle$, and $|+\beta\rangle,\ |-\beta\rangle$. (5)

The probability of detecting two coincident photons (simultaneous detections at both detectors) with the same (or opposite) polarization is given by (Barnett, 2009; Kudinoor & Suryanarayanan, 2022)

$P_{\pm\pm}(\alpha,\beta) = |\langle\pm_\alpha|\langle\pm_\beta|\Phi^+\rangle|^2$. (6)

These probabilities are used to compute the correlation value $E(\alpha,\beta)$ using the following formula

$E(\alpha,\beta) = P_{++}(\alpha,\beta) + P_{--}(\alpha,\beta) - P_{+-}(\alpha,\beta) - P_{-+}(\alpha,\beta)$. (7)

From the theory, the predicted correlation is (Barnett, 2009)

$E(\alpha,\beta) = cos(2(\alpha-\beta))$ (8)

The correlation values obtained from four different angle settings, $\alpha, \beta, \alpha', and\ \beta'$, are used to determine the CHSH inequality parameter S:

$S = E(\alpha,\beta) - E(\alpha',\beta) + E(\alpha,\beta') + E(\alpha',\beta')$ (9)

In accordance with the local hidden variable theory, this value must satisfy the CHSH inequality, $|S| \leq 2$. The experimental results violating the inequality such that, $|S| > 2$, reflects the nonlocal nature of quantum entanglement (Kudinoor & Suryanarayanan, 2022).

The maximum violation occurs when the angle differences are chosen to be

$\beta - \alpha = \alpha' - \beta = \beta' - \alpha' = 22.5°$

$\beta' - \alpha = 67.5°$.

In such a case, the theoretical maximum value of $|S|$ is:

$|S|_{max} = 2\sqrt{2} \approx 2.828$ (10)

Which clearly exceeds the bound of 2, thus serving as strong theoretical evidence of quantum nonlocality.

In the next section, we demonstrate the experimental results and determine whether they agree with these theoretical predictions in Equation 10.

The correlation value $E_{(\alpha,\beta)}$ can also be calculated from the coincidence counts of detected photons as

$E_{(\alpha,\beta)} = \frac{C_{++}-C_{-+}-C_{+-}+C_{--}}{C_{++}+C_{-+}+C_{+-}+C_{--}}$, (11)

Where C_{ij} represents the coincidence counts of the photons in positive and negative polarization states, written in equation (5).

The uncertainty in the correlation $dE(\alpha,\beta)$ is calculated using Gaussian error propagation as

$\mathrm{d}E_{(\alpha,\beta)} = 2\frac{(C_{++}+C_{--})(C_{-+}+C_{+-})}{(C_{++}+C_{-+}+C_{+-}+C_{--})^2} \times \sqrt{\frac{1}{(C_{++}+C_{--})} + \frac{1}{(C_{-+}+C_{+-})}}$. (12)

The uncertainty of the |S| value is then given by

$\mathrm{d}|S| = \sqrt{\sum_{a=\alpha,\alpha';b=\beta,\beta'}(dE_{(a,b)})^2}$. (13)

RESULTS & DISCUSSION

From the measurement of polarization correlation of photon pairs, polarizer 1 was set at angles 0°, 45°, 90°, and 135°, respectively. For each angle of polarizer 1, the coincidence counts were measured by rotating polarizer 2 from 0 °to 360°. Coincidence count data were collected every 15 °of rotation angles. The graph representing the relation of coincidence counts and rotation angles is illustrated in Figure 4. The blue, yellow, green and red lines of the graph display the

coincidence counts at different rotation angles of polarizer 2 when polarizer 1 is rotated by α = 0, 45°, 90°, and 135 °respectively.

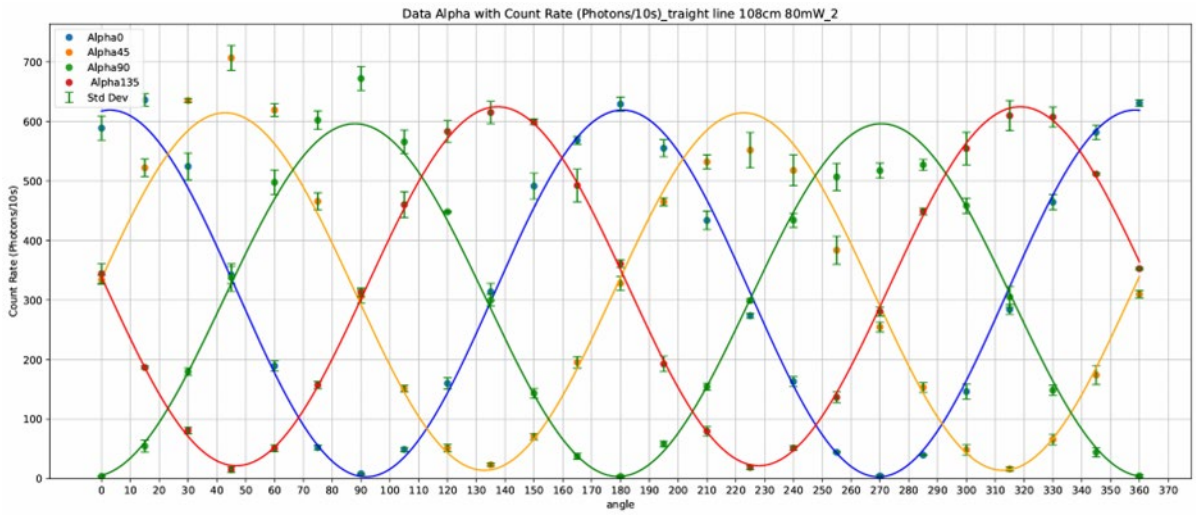

Figure 4 Coincidence counts at different rotated angles of polarizer 2. The blue, yellow, green and red lines represent the coincidence count at different rotation angles of polarizer 2 where the polarizer 1 is set at the angles α = 0°, 45°, 90° and 135° respectively. The data were fitted by the curves with the function $A + B\sin(\theta + \varphi)$.

In Figure 5, we plot the coincidence count data where polarizer 1 rotated by α = 45 ° together with the singles count data—collected from detector 2 by rotating polarizer 2 from 0 °to 360°, with the results recorded every 15° of rotation angles.

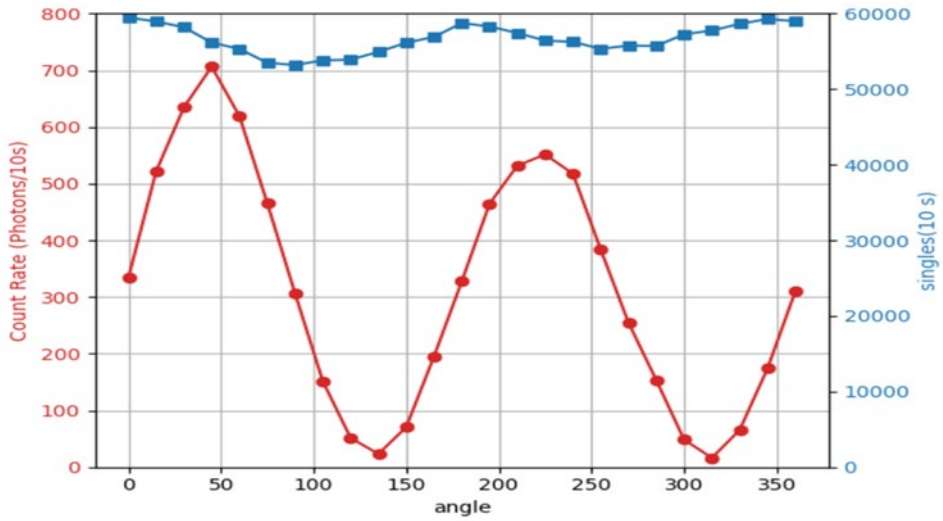

Figure 5 The graph shows the coincidence count rate (red) in the unit of photons/10s versus singles count (blue) in 10 s at the different rotation angle of polarizer 2.

The results from Figure 5 apparently show that the singles count (blue line) does not significantly change with respect to the rotation angles of the polarizer 2 compared with the coincidence counts (red line) (Kwiat, 1999). The difference between the blue and red lines clearly demonstrates a strong correlation between the photon pairs.
Based on the data presented in Figure 4, the CHSH's inequality value was calculated, and its results are presented in Table 1.

Table 1 The measurement results for calculating the CHSH's inequality value

Polarization.1 (deg)	**Polarization.2 (deg)**	**Coincidence Count (photons/10second)**	**correlation value $E(\alpha,\beta)$**	**correlation $dE(\alpha,\beta)$**
$\alpha = 0.0$	$\beta = 22.5$	547.65		
$\alpha = 0.0$	$\beta_{\perp} = 112.5$	83.38		
$\alpha_{\perp} = 90.0$	$\beta = 22.5$	114.07	$E_{(\alpha,\beta)} = 0.68$	$dE_{(\alpha,\beta)} = 0.02$
$\alpha_{\perp} = 90.0$	$\beta_{\perp} = 112.5$	494.96		
$\alpha' = 45.0$	$\beta = 22.5$	541.97		
$\alpha' = 45.0$	$\beta_{\perp} = 112.5$	85.27		
$\alpha'_{\perp} = 135.0$	$\beta = 22.5$	121.68	$E_{(\alpha',\beta)} = 0.67$	$dE_{(\alpha',\beta)} = 0.02$
$\alpha'_{\perp} = 135.0$	$\beta_{\perp} = 112.5$	520.79		
$\alpha = 0.0$	$\beta' = 67.5$	18.76		
$\alpha = 0.0$	$\beta'_{\perp} = 157.5$	523.38		
$\alpha_{\perp} = 90.0$	$\beta' = 67.5$	526.86	$E_{(\alpha,\beta')} = -0.69$	$dE_{(\alpha,\beta')} = 0.02$
$\alpha_{\perp} = 90.0$	$\beta'_{\perp} = 157.5$	80.90		
$\alpha' = 45.0$	$\beta' = 67.5$	509.20		
$\alpha' = 45.0$	$\beta'_{\perp} = 157.5$	12.91		
$\alpha'_{\perp} = 135.0$	$\beta' = 67.5$	97.26	$E_{(\alpha',\beta')} = 0.66$	$dE_{(\alpha',\beta')} = 0.02$
$\alpha'_{\perp} = 135.0$	$\beta'_{\perp} = 157.5$	552.64		

Using Equations 9 and 13 and the data in table I, the violation of the CHSH's inequality is demonstrated with

$|S| = 2.709 \pm 0.083$.

It is only about 4% lower than the maximum value predicted by the theory. A significant excess of the value |S| over the local bound indicates a strong quantum entanglement between the down-converted photons, which is essential for the development of quantum communication applications.

CONCLUSION

The use of guiding laser with a paper mask in the setup process significantly improved the simplicity and precision of achieving photon correlation by reducing alignment errors, making the experimental procedure more accessible and reliable. This is confirmed by a clear violation of the CHSH inequality, with an observed value of S = 2.709 ± 0.083, confirming the strong quantum entanglement between photon pairs. Comparing to a rail-based arm method reported in (Boonkham & Limsuwan, 2019; Vest & Jacubowiez, 2022; Armendáriz & Velázquez, 2023), even though the rail-based arm method offers greater flexibility, making it more suitable for highly adjustable experiments, the our proposed method using paper mask becomes more advantageous for fixed SPDC configurations due to its high precision and stability, despite its limitation in flexibility. Moreover, the rail-based arm method requires a lot of effort in alignment as it is very sensitive to external disturbances.

REFERENCES

Armendáriz, G., & Velázquez, V. (2023). Determining single photon quantum states through robust waveguides on chip. *Photonics, 10*(7), 755.

Barnett, S. M. (2009). *Quantum information*. Oxford University Press.

Boonkham, K., & Limsuwan, P. (2019, November). A simple technique for measuring the spatial correlation of photon pairs for complete interference in the Michelson interferometer. In *Journal of Physics: Conference Series* (Vol. 1380, No. 1, p. 012043). IOP Publishing.

Gisin, N., Ribordy, G., Tittel, W., & Zbinden, H. (2002). Quantum cryptography. *Reviews of Modern Physics, 74*(1), 145-195.

Giovannetti, V., Lloyd, S., & Maccone, L. (2011). Advances in quantum metrology. *Nature Photonics, 5*(4), 222-229.

Horodecki, R., Horodecki, P., Horodecki, M., & Horodecki, K. (2009). The quantum entanglement. *Reviews of Modern Physics, 81*(2), 865.

Kimble, H. J. (2008). The quantum internet. *Nature, 453*(7198), 1023-1030.

Kudinoor, A., & Suryanarayanan, A. (2022). *Violating the CHSH inequality using entangled photons*. Columbia University-PHYS 3081 Intermediate Physics Laboratory.

Kwiat, P. G., Waks, E., White, A. G., Appelbaum, I., & Eberhard, P. H. (1999). Ultrabright source of polarization-entangled photons. *Physical Review A, 60*(2), R773-R776.

O'Brien, J. L., Furusawa, A., & Vučković, J. (2009). Photonic quantum technologies. *Nature Photonics, 3*(12), 687-695.

Scarani, V., Bechmann-Pasquinucci, H., Cerf, N. J., Dušek, M., Lütkenhaus, N., & Peev, M. (2009). The security of practical quantum key distribution. *Reviews of Modern Physics, 81*(3), 1301-1350.

Vest, B., & Jacubowiez, L. (2022). Quantum entanglement in the lab. *Photoniques, 113*, 26-31.

Xia, Y., Li, W., Clark, W., Hart, D., Zhuang, Q., & Zhang, Z. (2020). Demonstration of a reconfigurable entangled radio-frequency photonic sensor network. *Physical Review Letters, 124*(15), 150502.

Data Availability Statement: The raw data supporting the conclusions of this article will be made available by the authors, without undue reservation.

Conflicts of Interest: The authors declare that the research was conducted in the absence of any commercial or financial relationships that could be construed as a potential conflict of interest.

Publisher's Note: All claims expressed in this article are solely those of the authors and do not necessarily represent those of their affiliated organizations, or those of the publisher, the editors and the reviewers. Any product that may be evaluated in this article, or claim that may be made by its manufacturer, is not guaranteed or endorsed by the publisher.